IKAP localizes to membrane ruffles with filamin A and regulates actin cytoskeleton organization and cell migration

Lars Dan Johansen[1,*], Tiina Naumanen[1,*], Astrid Knudsen[1], Nina Westerlund[2], Irina Gromova[3], Melissa Junttila[2], Christina Nielsen[1], Trine Bøttzauw[1], Aviva Tolkovsky[4], Jukka Westermarck[2,5], Eleanor T. Coffey[2], Marja Jäättelä[1] and Tuula Kallunki[1,‡]

[1]Apoptosis Department and Center for Genotoxic Stress, Institute of Cancer Biology, Danish Cancer Society, Strandboulevarden 49, DK-2100 Copenhagen, Denmark
[2]Turku Centre for Biotechnology, Åbo Akademi and University of Turku, Turku, Finland
[3]Proteomics in Cancer, Institute of Cancer Biology, Danish Cancer Society, Copenhagen, Denmark
[4]Department of Biochemistry, University of Cambridge, Cambridge, UK
[5]Institute of Medical Technology, University of Tampere and Tampere University Hospital, Tampere, Finland
*These authors contributed equally to this work
‡Author for correspondence (e-mail: tk@cancer.dk)

Accepted 6 December 2007
Journal of Cell Science 121, 854-864 Published by The Company of Biologists 2008
doi:10.1242/jcs.013722

Summary

Loss-of-function mutations in the *IKBKAP* gene, which encodes IKAP (ELP1), cause familial dysautonomia (FD), with defective neuronal development and maintenance. Molecular mechanisms leading to FD are poorly understood. We demonstrate that various RNA-interference-based depletions of IKAP lead to defective adhesion and migration in several cell types, including rat primary neurons. The defects could be rescued by reintroduction of wild-type IKAP but not by FD-IKAP, a truncated form of IKAP constructed according to the mutation found in the majority of FD patients. Cytosolic IKAP co-purified with proteins involved in cell migration, including filamin A, which is also involved in neuronal migration. Immunostaining of IKAP and filamin A revealed a distinct co-localization of these two proteins in membrane ruffles. Depletion of IKAP resulted in a significant decrease in filamin A localization in membrane ruffles and defective actin cytoskeleton organization, which both could be rescued by the expression of wild-type IKAP but not by FD-IKAP. No downregulation in the protein levels of paxillin or beclin 1, which were recently described as specific transcriptional targets of IKAP, was detected. These results provide evidence for the role of the cytosolic interactions of IKAP in cell adhesion and migration, and support the notion that cell-motility deficiencies could contribute to FD.

Supplementary material available online at
http://jcs.biologists.org/cgi/content/full/121/6/854/DC1

Key words: Neuronal migration, Familial dysautonomia, ELP1, Paxillin, Beclin 1

Introduction

IκB-kinase-associated protein, IKAP, is a well-conserved 150-kDa protein that does not belong to any known protein family. Originally, IKAP was described as a scaffold protein for the IκB kinase (IKK) complex (Cohen et al., 1998). In the nucleus, IKAP, also known as the elongator protein 1 (Elp1 in yeast and ELP1 in human), is involved in RNA-polymerase-II-mediated transcriptional elongation by assembling the elongator-complex proteins (Otero et al., 1999; Hawkes et al., 2002). In the cytosol, in which the vast majority of IKAP resides, several functions for IKAP have recently been reported, such as involvement in Jun N-terminal kinase (JNK)-mediated stress signalling in human and in the regulation of exocytosis and transfer RNA (tRNA) modification in yeast (Holmberg et al., 2002; Rahl et al., 2005; Esberg et al., 2006).

Mutations in the *IKBKAP* gene, which encodes IKAP, cause the autosomal recessive neurodegenerative disease familial dysautonomia (FD) (Anderson et al., 2001; Slaugenhaupt et al., 2001). FD affects mainly the sensory and autonomous nervous systems, which display a decreased number of neurons because of a defect in neuronal development and maintenance (Axelrod, 2004). The vast majority of FD (99.5% of cases) is caused by a loss-of-function mutation in the *IKBKAP* gene due to a single point mutation, which leads to variable skipping of exon 20. As a result, a 3′-end-truncated mRNA transcript of *IKBKAP* is expressed at variable levels in different tissues together with full-length *IKBKAP* (Slaugenhaupt et al., 2001; Anderson et al., 2001). The pathogenic result of the *IKBKAP* splice mutation is a tissue-specific reduction of wild-type IKAP protein below a tolerable threshold in the sensory and autonomous nervous systems (Slaugenhaupt et al., 2001; Cuajungco et al., 2003; Hims et al., 2007). It is not known whether the truncated IKAP transcript resulting from the exon skipping is degraded or whether it is translated into a C-terminally truncated IKAP protein termed here as FD-IKAP. According to existing theory, it is believed that the mutant message would not be translated but instead would be targeted for nonsense-mediated decay (Slaugenhaupt et al., 2004).

Filamin A organizes cortical actin filaments and dynamic three-dimensional networks in the leading edges of migrating cells (Feng and Walsh, 2004). Filamin A also interacts with various membrane proteins and intracellular mediators of adhesion and migration, and serves as a mechanical element in membrane ruffle formation (Vadlamudi et al., 2002; Popowicz et al., 2006). Loss-of-function

Journal of Cell Science

mutations of filamin A cause human periventricular heterotopia, an X-linked neurodevelopmental disorder. The disease is caused by a failure of neurons to migrate to the cortex, illustrated by the accumulation of neuronal cell bodies along the lateral ventricles (Fox et al., 1998).

To establish a cellular model system in which to study the function(s) of IKAP that could account for the development of FD, we prepared small interference RNA (siRNA)- and short hairpin RNA (shRNA)-based RNA interference (RNAi) systems using several non-overlapping *IKBKAP* mRNA sequences for the depletion of endogenous IKAP in human, rat and mouse cells. Analysis of various IKAP-depleted cells and rat primary neurons revealed decreased cell adhesion and migration, which both could be rescued by IKAP but not by FD-IKAP, which was found to be stably expressed in all tested cell lines. By affinity purification, the cytosolic pool of IKAP was found to associate with several proteins, of which filamin A was further studied because of its role in neuronal migration. Immunostaining of IKAP and filamin A revealed a distinct co-localization of these two proteins at membrane ruffles in the leading edge of the migrating cells. Depletion of IKAP resulted in decreased staining of filamin A in membrane ruffles and in disorganized actin cytoskeleton. Together, these data provide evidence for the general involvement of IKAP in cell adhesion and migration via cytosolic interactions, and suggest a novel cellular mechanism of how loss-of-function mutations of IKAP could contribute to FD.

Results

IKAP is involved in cell spreading, adhesion and migration

Two retroviral shRNA constructs were made against murine *IKBKAP* (m1 and m2), and three retroviral shRNA constructs (h1, h2 and h3) and one siRNA oligonucleotide (H1) were made against human *IKBKAP* (supplementary material Fig. S1). Western blot analysis of IKAP from cells treated with any of the five different retroviral shRNA constructs or with the one siRNA oligonucleotide showed pronounced depletion of IKAP as compared with the corresponding vector-control-treated or scrambled (scr)-siRNA-oligonucleotide-treated cells (Fig. 1A; supplementary material Fig.

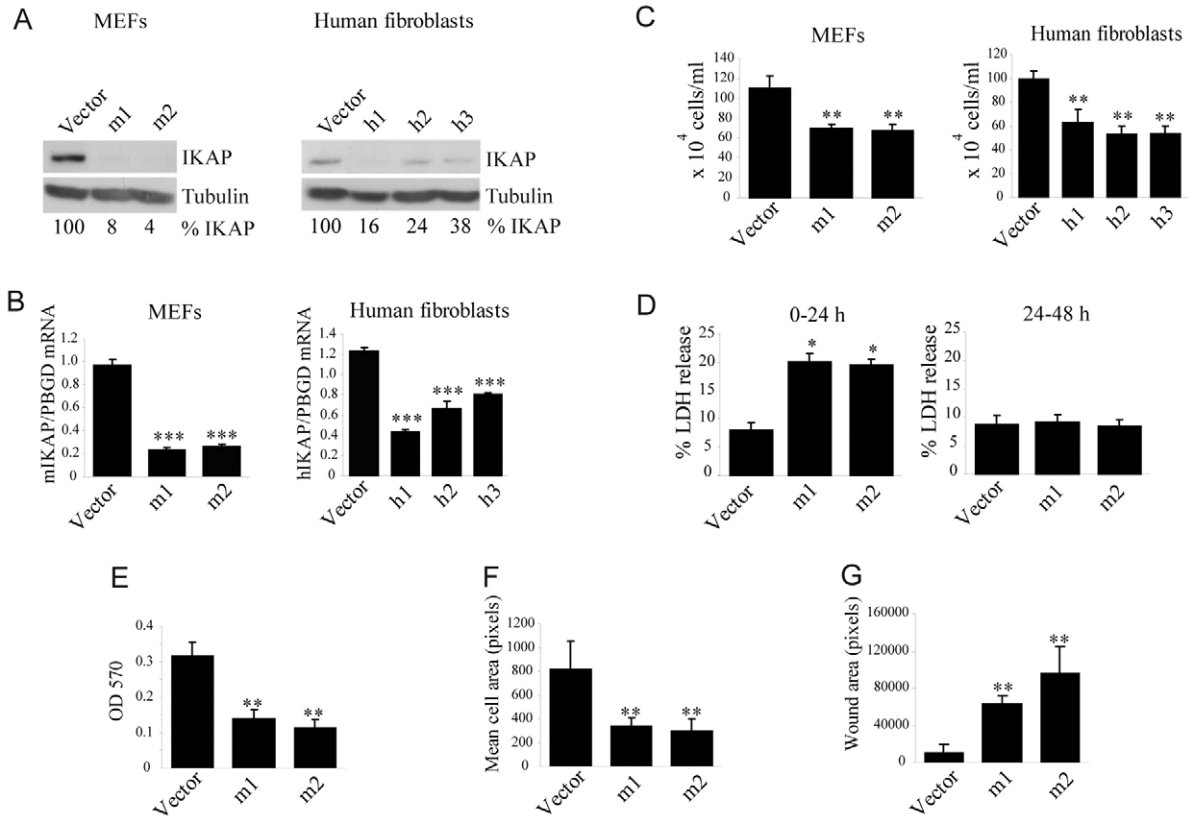

Fig. 1. RNAi depletion of IKAP results in decreased plating efficiency, cell adhesion, spreading and migration. (A) Western blot analysis of *IKBKAP*-shRNA-transduced MEFs (m1 and m2) and human fibroblasts (h1-h3) after antibiotic selection. % IKAP values represent the quantification of IKAP depletion in human fibroblasts (n=2) and MEFs (n=3). (B) RT-PCR analysis of *IKBKAP*-shRNA-treated MEFs (means ± s.d.; n=3; triplicates; ***P<0.001) and human fibroblasts (means ± s.d.; n=1; triplicates; ***P<0.001) after antibiotic selection. (C) Evaluation of plating efficiency. Cells were inoculated with a density of 1.5×10^4 cells/ml for MEFs or 2×10^4 cells/ml for human fibroblasts and analyzed 24 hours later. Calculation of cell numbers (means ± s.d.; n=3; triplicates; **P<0.01). (D) The level of cell death in designated MEFs was investigated by measuring LDH release 24 hours after plating and again 24 hours later after a change of media (means ± s.d.; n=1; triplicates; *P<0.05). (E) The adhesion of MEFs was analyzed by inoculating 5×10^4 cells/ml in serum-free media on non-supporting adherent-surface 24-well plates (Sarstedt) for 1.5 hours. Cells were washed with PBS and fixed for 10 minutes with crystal violet stain [CV; 0.5% crystal violet (Sigma) containing 25% methanol]. The excess dye was rinsed off, the cells were re-suspended in Na-citrate buffer (0.1 M Na-citrate, 50% ethanol) and the absorbance (OD) at 570 nm was measured (means ± s.d.; n=3; triplicates; **P<0.01). (F) To analyze cell spreading, CV-stained cells were imaged by 20× magnification on an Olympus IX70 inverted microscope with an Olympus C-5050 digital camera. The cell areas were measured using ImageJ software (http://rsb.info.nih.gov/ij/) and divided by the number of cells present (means ± s.d.; n=3; triplicates; **P<0.01). (G) For cell migration study, the cells were seeded at a density of 1×10^5 cells/ml and allowed to adhere over night. A wound was inflicted by scraping a 200 μl sterile tip across the cell layer. The cells were incubated for 17 hours followed by imaging at 10× magnification on an Olympus IX70 inverted microscope with an Olympus C-5050 digital camera. Average wound area was quantified in the picture using ImageJ software (means ± s.d.; n=3; **P<0.01).

Journal of Cell Science

S2A). Depletion was further verified by reverse transcriptase (RT)-PCR (Fig. 1B). Interestingly, the confluence of IKAP-depleted cultures appeared clearly reduced as compared with the control cultures in all cell lines at 24 hours after plating. IKAP-depleted cultures had 40% fewer cells than the corresponding control cultures (Fig. 1C; supplementary material Fig. S2B).

Growth-rate and cell-cycle-phase analysis revealed that the depletion of IKAP did not alter cellular growth (supplementary material Fig. S2C). The amount of lactate dehydrogenase (LDH) released from the cytosol into tissue culture media was increased in IKAP-depleted cells, indicating plasma membrane rupture and cell death, as measured at 24 hours after plating (Fig. 1D, left-hand graph). Cell death was limited to the post-plating period and did not increase during the second day of culture with the change of media after the first 24 hours (Fig. 1D; right-hand graph), suggesting that the sparser appearance of the IKAP-depleted cells observed 24 hours after plating was due to poorer plating efficiency and not due to decreased cell survival. This was also supported with the apparent lack of a sub-G1 fraction in flow cytometric analysis of propidium iodide (PI)-stained cells that were allowed to grow for at least 24 hours after the media change (supplementary material Fig. S2C). Consequently, experiments assessing the ability of cells to adhere to a non-supporting adherent surface revealed that cell adhesion was severely deficient in IKAP-depleted cells (Fig. 1E). The poorer adhesion properties were associated with a measurable defect on the spreading of these cells (Fig. 1F). A wound-healing assay revealed a slower migrating phenotype in IKAP-depleted cells when compared with control cells (Fig. 1G), as reported previously (Close et al., 2006). Consistent with the previous study, no effect in stress-induced JNK activity was detected upon depletion of IKAP (data not shown). All the phenotypes observed in mouse embryonic fibroblasts (MEFs) could also be detected in *IKBKAP*-siRNA-treated HeLa cells (supplementary material Fig. S2B,D-G).

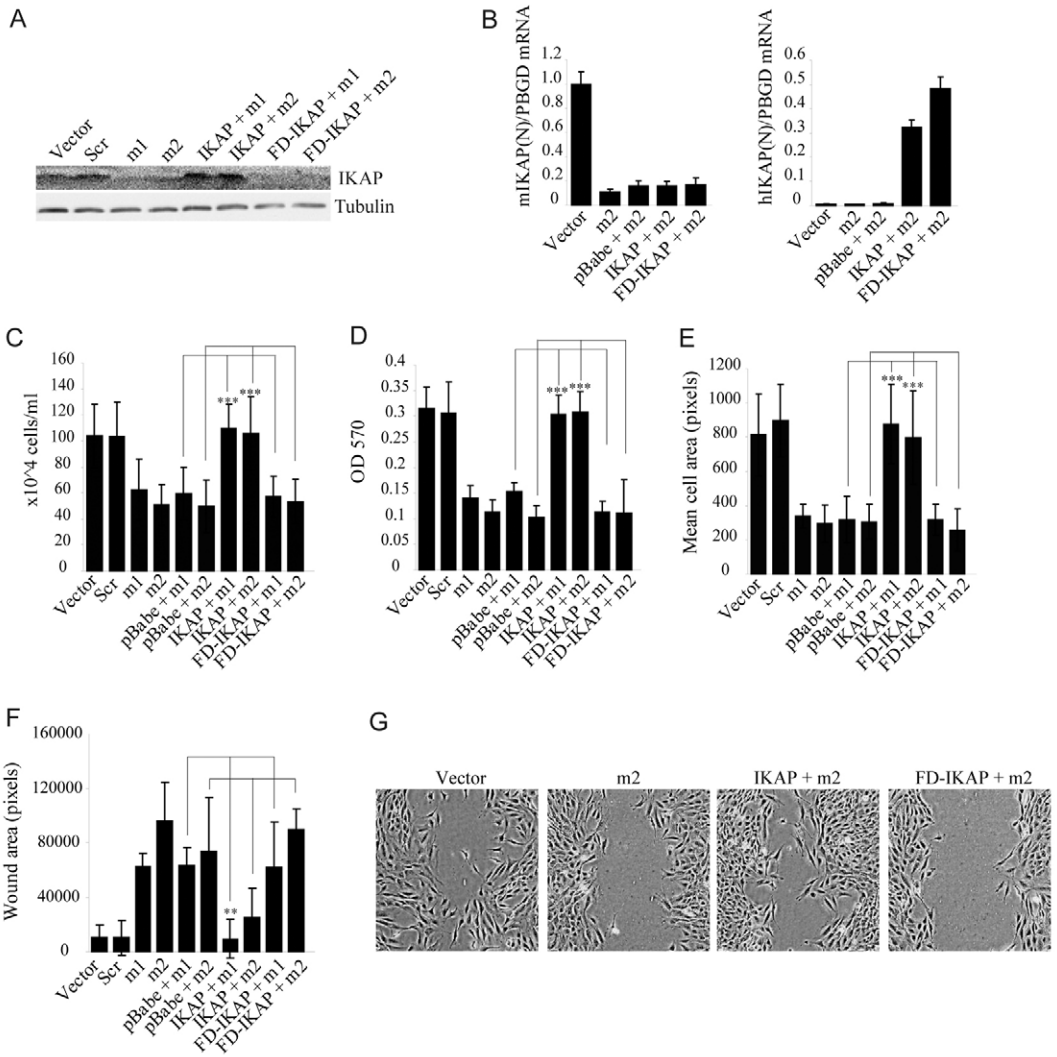

Fig. 2. Reintroduction of human IKAP but not FD-IKAP rescues the plating efficiency, cell adhesion, spreading and migration phenotypes of IKAP-depleted MEFs. (A) Western blot analysis of IKAP-depleted MEFs (m1 and m2) with the reintroduction of wild-type IKAP and FD-IKAP. (B) RT-PCR analysis of *IKBKAP* in MEFs after IKAP depletion by shRNA and reintroduction of wild-type IKAP or FD-IKAP. Left, RT-PCR with oligonucleotides recognizing mouse IKBKAP; right, RT-PCR with oligonucleotides recognizing the 5′ end of the human *IKBKAP* reintroduced to MEFs. (C) Plating efficiencies; (D) adhesion; (E) spreading; and (F) migration properties of the MEFs upon IKAP depletion (m1 and m2) and reintroduction of designated IKAP expression constructs together with corresponding empty vector (vector), scrambled (Scr) and protein expression vector pBabe controls were analyzed as in Fig. 1 (means ± s.d.; n=3; triplicates; $^{**}P<0.01$; $^{***}P<0.001$). (G) Phase-contrast images of the designated wound-healing assays carried out as described in Fig. 1G.

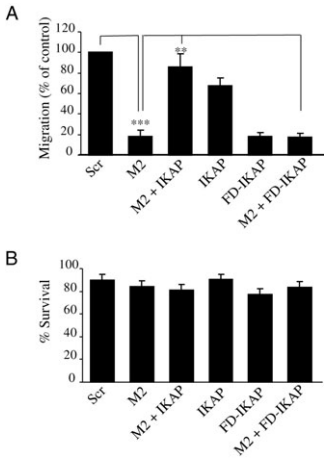

Fig. 3. RNAi depletion of IKAP results in migration defects in rat cerebellar granule neurons that can be rescued by full-length but not FD-IKAP. (A) Migration of cerebellar granule neurons transiently transfected with designated *IKBKAP* (M2) or scr siRNA oligonucleotide and/or *IKBKAP* plasmids was quantified and normalized to control levels (means ± s.d.; n=4; $^{**}P<0.01$; $^{***}P<0.001$). (B) Viability of neurons expressing designated *IKBKAP* or scr siRNA and/or *IKBKAP* plasmids (means ± s.d.; n=4).

All experiments using shRNAs were performed with freshly transduced pooled cells. Because of severe adhesion problems of IKAP-depleted cells, which led to the loss of the cells having most efficient IKAP depletion upon each cell passage, in all following experiments, MEFs were only used up to passage 5 after transduction.

Reintroduction of wild-type IKAP but not FD-IKAP rescues the impairments in cell adhesion, spreading and migration of IKAP-depleted MEFs and rat cerebellar granule neurons

Next, we studied whether IKAP and FD-IKAP have separable abilities to regulate cell adhesion and migration. We introduced human IKAP expression constructs into MEFs depleted of IKAP. Human and mouse IKAP proteins exhibit very small differences at their amino acid sequence. However, their mRNA sequences differ sufficiently so that the mouse *IKBKAP* shRNAs do not recognize ectopically introduced human wild-type IKAP, as investigated by western blot analysis (data not shown). The expression of human wild-type IKAP was confirmed by western blot (Fig. 2A). This method could not be applied to confirm the expression of the FD-IKAP construct, because of the lack of antibodies against the N-terminus of IKAP that would function in western blot analysis. Instead, RT-PCR was used to confirm the expression of the FD-*IKBKAP* mRNA (Fig. 2B). The m2-shRNA-expressing MEFs that were transduced with the retroviral human *IKBKAP*, FD-*IKBKAP* or control construct exhibited marked depletion of murine *IKBKAP* mRNA, as analyzed by RT-PCR using the mouse *IKBKAP*-specific primer set (Fig. 2B; left-hand graph). The FD-*IKBKAP* construct was clearly detectable in the RT-PCR with the human N-terminal-*IKBKAP*-specific PCR primer set, which expectedly also recognized the human wild-type *IKBKAP* (Fig. 2B; right graph). Importantly, complete rescue of the plating efficiency (Fig. 2C), cell adhesion (Fig. 2D), spreading (Fig. 2E) and migration (Fig. 2F,G) was achieved by expressing human IKAP in MEFs with depleted murine IKAP, verifying the specificity of the hairpins. Notably, the expression of FD-IKAP did not rescue any of these phenotypes (Fig. 2C-G). These data show that IKAP but not FD-IKAP can rescue IKAP-depleted MEFs from the defect-phenotypes observed.

To investigate the effect of IKAP depletion on the survival and migration of rat primary neurons, we prepared an M2 siRNA oligonucleotide against rat and mouse *IKBKAP* according to the mouse shRNA construct m2. We chose cerebellar granule neurons for analysis of neuronal migration because they are amenable to in vitro investigation and provide a well-characterized model that closely mimics neuronal migration in vivo (Rakic et al., 1974; Hatten, 1990). Transfection of the M2 siRNA oligonucleotide into rat cerebellar granule neurons resulted in a severe migration impairment, which could be fully rescued by ectopic expression of wild-type IKAP (Fig. 3A). As expected, FD-IKAP could not rescue the migratory defect of the IKAP-depleted neurons. Interestingly, mere overexpression of FD-IKAP resulted in a severe neuronal migration defect, suggesting that its overexpression even in the presence of endogenous IKAP can inhibit neuronal migration. The introduction of *IKBKAP* siRNA or *IKBKAP* expression constructs did not affect neuronal survival (Fig. 3B). These results demonstrate that IKAP is generally involved in cell adhesion and migration, and specifically in neuronal migration, and that expression of FD-IKAP both in the presence or absence of wild-type IKAP can cause a severe defect in neuronal migration.

IKAP depletion affects distribution of paxillin and vinculin and organization of actin stress fibers with no evidence for changes in the protein levels of these three proteins

Next, we compared the distribution of vinculin, paxillin and actin in IKAP-depleted and control cells. At 1.5 hours after plating, IKAP-depleted cells showed a remarkable defect in the distribution of paxillin and vinculin at the focal contact points in comparison to the corresponding vector control cells; this defect could be reverted by reintroduction of human IKAP but not FD-IKAP into murine IKAP-depleted cells (Fig. 4A). Quantitation of cells with normal paxillin distribution at focal adhesions (% positive cells) revealed a defect in paxillin distribution in m2-shRNA-treated cells as well as in its rescue by IKAP, which were both significant (Fig. 4B). Still, at 24 hours after plating, IKAP-depleted cells showed a clear loss of organization of actin stress fibers, even though they were fully spread on the surface, as were the control cells (Fig. 4A, bottom panels). Quantification of the cells with organized actin stress fibers (% positive cells) revealed that the control cells exhibited approximately three times as many cells with organized actin fibers than the IKAP-depleted cells and again ectopic IKAP but not FD-IKAP could rescue the defective actin organization (Fig. 4C). Western blot analysis revealed no changes in vinculin, paxillin or actin levels in IKAP-depleted cells (Fig. 4D). Analysis of the ratio of soluble actin (S; G-actin) in comparison to insoluble actin (I; F-actin) revealed no difference between IKAP-depleted and control cells, suggesting that the depletion of IKAP was not affecting F-actin turnover (Fig. 4E).

A recent study based on depletion of IKAP with a single RNAi sequence (Close et al., 2006) showed marked paxillin and beclin 1 mRNA depletion and modest α-tubulin mRNA upregulation in IKAP-depleted HeLa cells and human fibroblasts, as well as modest downregulation of the paxillin protein in HeLa cells. Surprisingly, we did not observe any difference in the protein levels of either paxillin or beclin 1 in IKAP-depleted MEFs or HeLa cells (Fig. 4D). Comparison of paxillin and beclin 1 levels in fibroblasts isolated from an FD patient and a control individual failed to reveal any differences in the levels of these proteins (Fig.

Journal of Cell Science

Journal of Cell Science

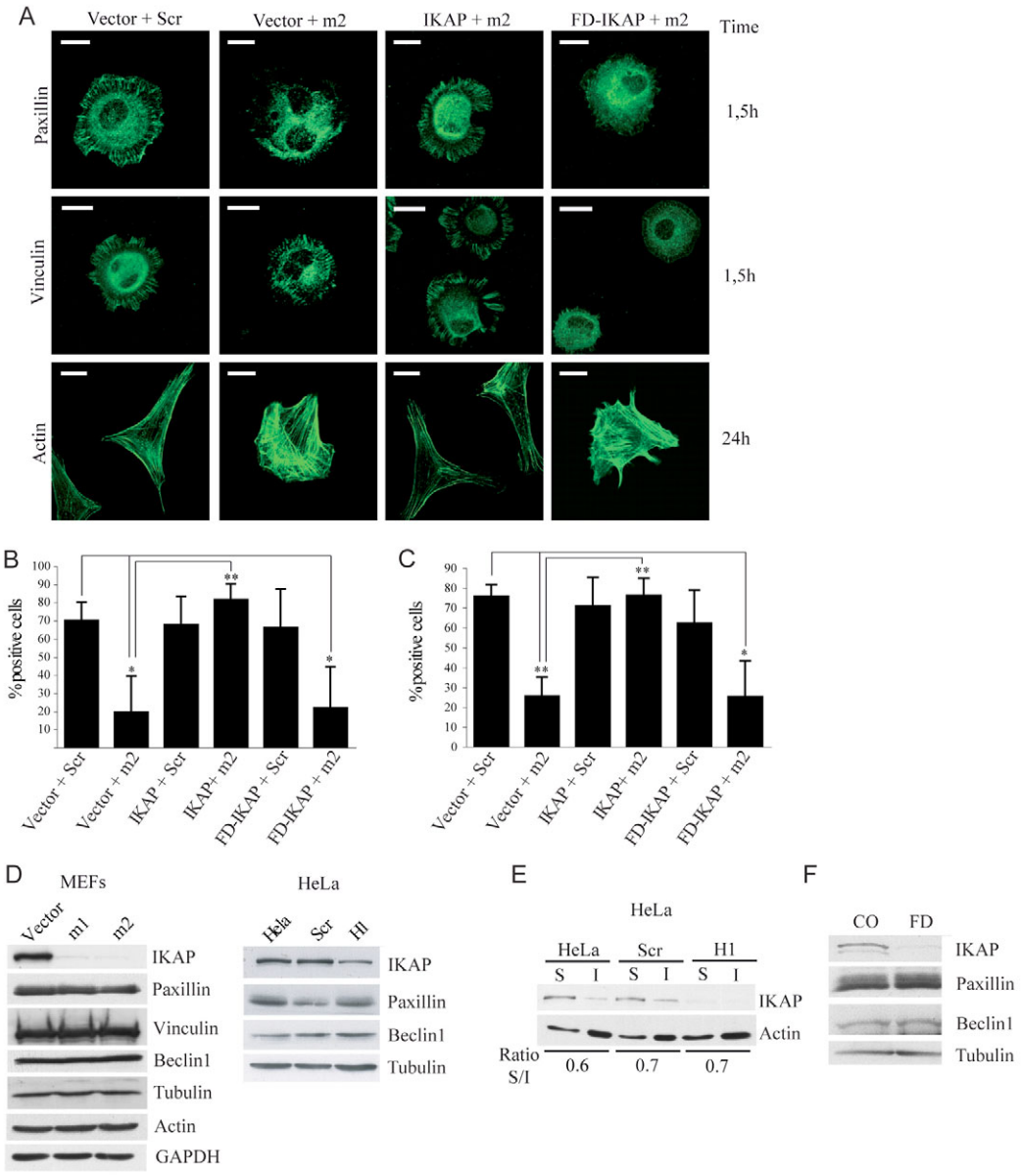

Fig. 4. Focal adhesion and actin organization is disturbed in IKAP-depleted MEFs. (A) IKAP-depleted (m2) or control (scr) MEFs were stained for paxillin and vinculin at 1.5 hours after plating and for actin at 24 hours. Human IKAP or FD-IKAP was introduced to some of the murine IKAP-depleted cells as indicated. (B) Quantification of the number of cells with organized paxillin staining (means ± s.d.; n=3; $^{**}P$<0.01). (C) Quantification of the percentage of cells with organized actin cytoskeleton (means ± s.d.; n=3; $^{**}P$<0.01). (D) Western blot analysis of protein levels in MEFs transduced with designated *IKBKAP* shRNA constructs (left panel) or HeLa cells transiently transfected with siRNA oligonucleotides (right panel) for 48 hours. (E) The soluble (S; G-actin) and insoluble (I; F-actin) actin content of HeLa cells transiently expressing H1 *IKBKAP* siRNA or scr control oligonucleotide was assessed by western blotting. Triton X-100 soluble and insoluble proteins were extracted as described in the Materials and Methods, and lysates were analyzed for IKAP and β-actin. The quantification was made by ImageGauge software. The quantification is representative of two independent experiments. (F) Paxillin and beclin 1 protein levels in western blot analysis of FD-patient fibroblasts and fibroblasts from a healthy control individual. Scale bars: 20 μm.

4F). To explore the possible transcriptional effects resulting from the depletion of IKAP, we performed expression array analysis with an array specific for mRNAs of proteins involved in adhesion and migration. Comparison of the data obtained from IKAP-depleted and vector control cells did not reveal any significant transcriptional differences between these two samples except for NCAM (supplementary material Fig. S3A). The reduction in NCAM signal was, however, not accompanied by a decrease in NCAM protein levels (supplementary material Fig. S3B). These results strongly suggest that IKAP is required for actin cytoskeleton organization and that the cell-migration defects observed in IKAP-depleted cells are unlikely to be mediated by changes in the transcriptional regulation of genes most commonly involved in adhesion or migration.

IKAP interacts with cytosolic proteins involved in cell migration

Because the majority of IKAP is localized to the cytosol (Holmberg et al., 2002; Krogan et al., 2002; Pokholok et al., 2002; Rahl et al., 2005) and because no transcriptional defects that could explain the phenotype of the IKAP-depleted cells were observed, we screened

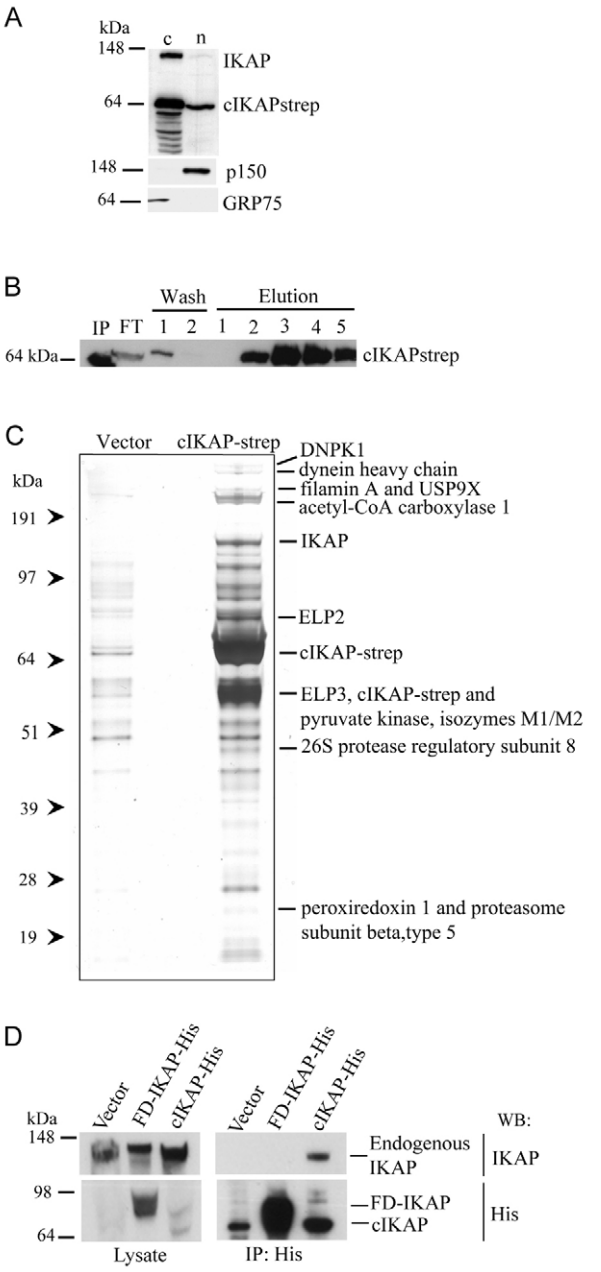

Fig. 5. IKAP co-purifies with various cytosolic proteins. (A) Western blot analysis of equal amounts of proteins from cytosolic and nuclear fractions of cIKAP-strep-expressing HEK293 cells. Anti-IKAP antibody was used to detect endogenous IKAP and cIKAP-strep. Western blot analysis of p150 and GRP75 were used to control the purity of the nuclear and cytosolic extracts, respectively. (B,C) One-STrEP-tag purification. HEK293 cells transiently transfected with either empty vector or cIKAP-strep were harvested 2 days after transfection and cytosolic extracts were prepared as described in the Materials and Methods. Purification was performed according to the manufacturer's instructions (IBA). Eluates were concentrated and run on 10% SDS-PAGE. (B) Western blot analysis of cIKAP-strep detected by anti-IKAP antibody in different purification steps. IP, input; FT, flow through. (C) Silver staining of the purified proteins. The indicated proteins were identified by MALDI-TOF-MS. DNPK1, DNA-dependent protein kinase; USP9X, ubiquitin-specific processing protease. (D) Association of IKAP with its C-terminus. HEK293 cells were transiently transfected with either empty vector, or with FD-IKAP-His or cIKAP-His constructs. After 48 hours, cytosolic extracts were prepared and immunoprecipitated with anti-His antibody. Immunoprecipitates were run on SDS-PAGE and analyzed for endogenous IKAP and the His-tagged IKAP fragments.

for the possible cytosolic interaction partners of IKAP. As bait we used the C-terminus of IKAP (C-IKAP), missing from the FD-IKAP, assuming that it might contain sequences important for the function of IKAP. C-IKAP (aa 715-1332) was cloned into pEXPR-IBA105 mammalian expression vector (designated here as cIKAP-strep) in order to take advantage of the one-STrEP-tag affinity-purification method that allows purification of associating proteins under physiological conditions (Junttila et al., 2005). We confirmed that the majority of the cIKAP-strep (64 kDa) localized to the cytosolic fraction, as did the endogenous IKAP (150 kDa) (Fig. 5A). Cytosolic fractions were extracted from HEK293 cells expressing cIKAP-strep or corresponding vector control and used for STrEP-tag affinity purification. The enrichment of cIKAP-strep during the purification steps was verified (Fig. 5B). The proteins co-purifying with cIKAP-strep were visualized by silver staining followed by identification with matrix-assisted laser desorption/ionization time-of-flight (MALDI-TOF) mass spectrometry (Fig. 5C). A total of 15 proteins were found to associate specifically with the bait in two purification experiments (Table 1). Surprisingly, endogenous IKAP co-purified with cIKAP-strep (Fig. 5C). This was verified by co-immunoprecipitation using ectopically expressed His-tagged cIKAP (cIKAP-His) and FD-IKAP-His, of which only cIKAP-His associated with endogenous IKAP (Fig. 5D). Interestingly, four (excluding IKAP itself) out of the 15 associating proteins had previously been linked to cell migration in general and only two to neuronal migration; filamin A and dynein heavy chain (Fig. 5C; Table 1). Furthermore, elongator-complex proteins Elp2 and Elp3 co-purified with cIKAP-strep (Fig. 5C), suggesting that these two proteins also reside in cytosol. This supports the earlier observations of cytosolic localization of human ELP2 (Collum et al., 2000) and yeast Elp2 and Elp3 (Rahl et al., 2005; Esberg et al., 2006). Taken together, these results demonstrate that IKAP interacts with itself and with various cytosolic proteins, two of which are involved in neuronal migration.

IKAP co-localizes with filamin A into membrane ruffles

Of the purified IKAP-associating proteins, filamin A was especially interesting because, in addition to regulating neuronal migration, it is also involved in a neurodevelopmental disorder called periventricular heterotopia (Fox et al., 1998), which involves defective neuronal migration. To examine whether filamin A is expressed in sympathetic neurons (SCG) that are affected in FD, RT-PCR was set up to detect filamin A mRNA. RT-PCR revealed both filamin A and *IKBKAP* expression in these neurons (Fig. 6A). Amplification of vasoactive intestinal peptide (*VIP*) was used to demonstrate the specificity of the neuronal preparation (Fann and Patterson, 1993; Habecker et al., 1997). We therefore chose to investigate the possible interaction between IKAP and filamin A. HEK293 cells expressing filamin A together with either His-tagged IKAP or empty vector were lysed and immunoprecipitated with anti-His antibody. Western blot analysis of the precipitates for IKAP and filamin A verified that filamin A co-immunoprecipitated with IKAP (Fig. 6B). In these assays it became clear that the IKAP-association site was located in the N-terminus of filamin A, because the co-precipitated filamin A corresponded to its 190 kDa calpain-cleaved N-terminal fragment (Fig. 6B) (Kiema et al., 2006). Association of filamin A with IKAP was indirect, because in-vitro-translated N-terminal filamin A did not bind IKAP (Fig. 6C). We investigated the possible co-localization of IKAP and filamin A by performing co-immunostaining in IKAP-depleted and control MEFs. We used an antibody (422) that we developed against the

Table 1. Function of proteins found to associate with IKAP by affinity purification

Protein	Accession[1]	Localization[2]	Function[3]	Function in migration
DNPK1	P78527	Nucleus	Signal transduction	
Dynein heavy chain	Q14204	Cytoplasm	Microtubule motor	*[4], **[5]
Filamin A	P21333	Cytoplasm	Cell motility	*[6], **[7]
USP9X	Q93008	Cytoplasm	Deubiquitylation	*[8]
Acetyl-CoA carboxylase 1	Q13085	Cytoplasm	Fatty acid biosynthesis	
IKAP	O95163	Cytoplasm	Multifunctional, migration	*[9]
ELP2	AAK97355	Cytoplasm	Transcription elongation	
ELP3	NP_060561	Cytoplasm	Acyltransferase	
Pyruvate kinase	P14618	Cytoplasm	Glycolysis	
PSMC5	P62195	Cytoplasm	Proteasomal degradation	
Peroxiredoxin 1	Q06830	Cytoplasm	Cell proliferation	
PSMB5	P28074	Cytoplasm	Proteasomal degradation	
BMX	NP_001712	Cytoplasm	Signal transduction	*[10]
MYLK2	Q9H1R3	Cytoplasm	Myosin phosphorylation	
DNAJB11	Q9UBS4	ER	Chaperone	

[1]Accession number for SwissProt or NCBI; [2]localization of the proteins are given according to HPRD or SwissProt; [3]protein functions are given according to the primary function in GO or SwissProt; [4](Dujardin et al., 2003); [5](Sasaki et al., 2000); [6](Cunningham et al., 1992); [7](Fox et al., 1998); [8](Friocourt et al., 2005); [9](Close et al., 2006); [10](Abassi et al., 2003).

*Function in migration has been shown in some cells; **function in migration in neurons has been shown.

DNPK1, DNA-dependent protein kinase, catalytic subunit; USP9X, ubiquitin-specific processing protease; ELP2, elongator protein 2; ELP3, elongation protein 3 homolog; PSMC5, 26S protease regulatory subunit 8; PSMB5, proteasome subunit beta, type 5; BMX, non-receptor tyrosine kinase; MYLK2, myosin-light-chain kinase 2; DNAJB11, DnaJ homolog subfamily B member 11; ER, endoplasmic reticulum.

N-terminus of IKAP to detect the expression of IKAP and FD-IKAP. This antibody is efficient in immunocytochemistry but does not work in western blots. Immunostaining revealed that IKAP and filamin A co-localized in membrane ruffles at the leading edges of migrating cells as well as in perinuclear areas (Fig. 6D). Filamin A localization to membrane ruffles (% positive cells) was approximately two times more common in scr controls than in IKAP-depleted (m2) cells (Fig. 6E), suggesting that IKAP could be involved in the regulation of filamin A localization into membrane ruffles. Ectopic expression of IKAP but not FD-IKAP rescued the filamin-A-localization defect in IKAP-depleted murine cells (Figs 6D,E). Moreover, expression of FD-IKAP was very visible in the cytosol at the perinuclear area, but was lacking from membrane ruffles (Fig. 6D). FD-IKAP was expressed as efficiently as wild-type IKAP, as determined from the staining of His-tag (Fig. 6F). No downregulation of the filamin A protein was observed in IKAP-depleted cells (Fig. 6H).

To verify the surprising observation of IKAP localizing to membrane ruffles, we stained MEFs and HeLa cells with three different anti-IKAP antibodies. All three antibodies gave rise to similar staining at perinuclear regions and at membrane ruffles (Fig. 6G). Ectopic expression of IKAP fused to the GFP (IKAP-GFP) also showed similar subcellular localization (Fig. 6G; lower rightmost image). Depletion of filamin A from the primary rat neurons also led to impaired migration (Fig. 6I) and the expression of filamin A siRNA was not toxic to the neurons (Fig. 6J). These results demonstrate that filamin A associates with IKAP and that, like IKAP, it is abundantly expressed in sympathetic neurons. IKAP co-localizes with filamin A to membrane ruffles and the localization of filamin A at the membrane ruffles is lost upon IKAP depletion. Furthermore, filamin A, which plays a crucial role in cortical neuron migration (Fox et al., 1998), seems to be required for migration of cerebellar granule neurons and its depletion from these neurons also leads to a migration defect.

Discussion

Divergent RNAi-based depletions of IKAP from different cell types, including primary rat neurons, resulted in defective cellular adhesion and migration without changes in the expression levels of adhesion- and migration-mediating proteins. Instead, IKAP was shown to associate with several proteins involved in migration, two of which, filamin A and dynein heavy chain, have a role in neuronal migration (Fox et al., 1998; Sasaki et al., 2000; Dujardin et al., 2003). As such, this work does not rule out the possibility that the depletion of IKAP could affect transcriptional elongation. Remarkably, however, it shows that the spreading, adhesion and migration defects resulting from IKAP depletion are achieved without downregulation of paxillin or beclin 1, which were suggested to be specific transcriptional targets of elongator (Close et al., 2006), or without several other key proteins known to be involved in cell adhesion or migration.

Introduction of human IKAP into IKAP-depleted MEFs or rat cerebellar granule neurons fully rescued the adhesion and migration defects resulting from IKAP depletion. Importantly, introduction of C-terminally truncated IKAP, here termed FD-IKAP, which was constructed according to the major mutation in *IKBKAP* in FD patients – a single base-pair change that leads to exon skipping, frame shift and expression of a truncated mRNA transcript, especially in the sensory and autonomous nervous system of the patients – could not rescue defects resulting from IKAP depletion. Notably, because of the lack of antibodies against the N-terminus of IKAP that function in western blotting, it is currently unclear whether FD patients express a truncated form of the IKAP protein (FD-IKAP) or whether the transcript is degraded by nonsense-mediated decay pathway (Slaugenhaupt et al., 2004). We show that His-tagged FD-IKAP is expressed and stable (Fig. 5D, Fig. 6F), as is the non-tagged FD-IKAP, which is evident from the clear increased perinuclear IKAP staining of FD-IKAP-introduced cells (Fig. 6D). Our data show that FD-IKAP cannot support the cell migration that is supported by wild-type IKAP. This could be due to the fact that FD-IKAP cannot localize to the leading edges of migrating cells. It is also possible that the dimerization/oligomerization of IKAP via its C-terminus, which is lacking from FD-IKAP, is necessary for the migration-supporting function of IKAP. Overexpression of FD-IKAP in cerebellar granule neurons led to a severe migratory defect, suggesting that FD-IKAP could

Journal of Cell Science

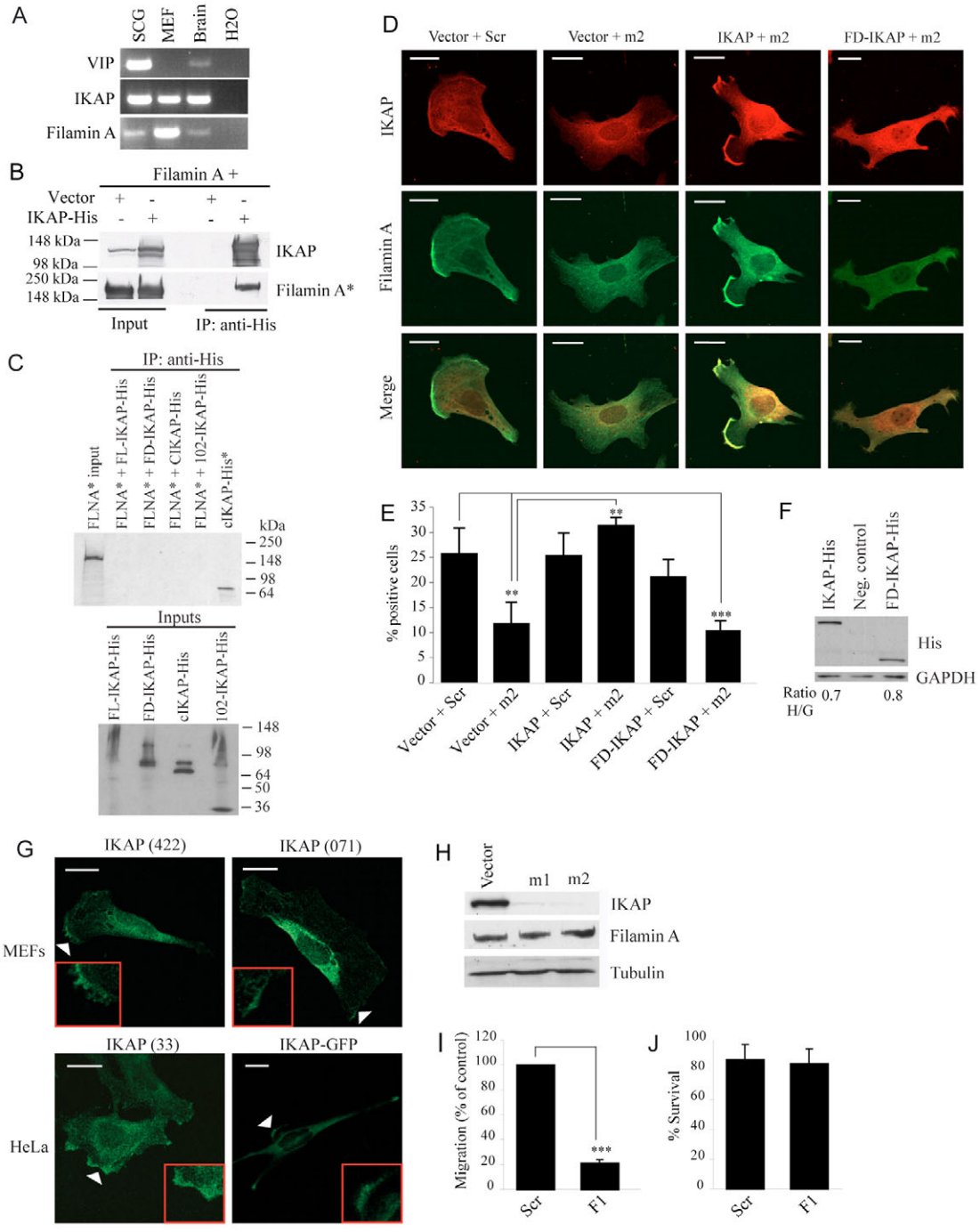

Fig. 6. IKAP co-localizes with filamin A into membrane ruffles. (A) RT-PCR of *IKBKAP*, *VIP* and filamin A. cDNA was prepared from RNA isolated from rat sympathetic neurons (SCG), MEFs and mouse brain. Water was used as a negative control. (B) IKAP association with filamin A. HEK293 cells were transiently transfected with filamin A together with either an empty vector or His-tagged full-length *IKBKAP*. After 48 hours, cytosolic extracts were prepared and immunoprecipitated with anti-His antibody. Immunoprecipitates were run on SDS-PAGE and analyzed for IKAP and filamin A. Asterisk indicates the 190-kD fragment of filamin A. (C) Pull-down experiment of in-vitro-translated IKAP and filamin A. Unlabeled His-tagged IKAP fragments, S35-labeled (*) N-terminal filamin A fragments and cIKAP-His were in vitro translated with TNT T7 coupled reticulosate lysate system (Promega). Designated in vitro translations were combined and pulled down with anti-His antibody. Upper panel, autoradiogram of pull downs; lower panel, western blot of the IKAP inputs with anti-His antibody. (D) IKAP and filamin A co-immunostaining in IKAP-depleted (m2) and control (scr) MEFs. Human wild-type IKAP and FD-IKAP were expressed in murine IKAP-depleted MEFs as indicated. Cells were plated on coverslips for 24 hours, fixed and stained. (E) Quantification of the percentage of cells with filamin A staining at the membrane ruffles (means ± s.d.; n=3; $^{**}P$<0.01). (F) Western blot analysis of IKAP and FD-IKAP expression. The quantification (His versus GAPDH; H/G) is representative of two independent transfections. (G) Immunostaining of cells using three different anti-IKAP antibodies (upper panels and lower leftmost panel) and image of the expression of IKAP-GFP in HeLa cells (lower rightmost panel). Boxed images show close-ups of the areas indicated by arrowheads. (H) Western blot analysis of filamin A expression in IKAP-depleted MEFs. (I) Migration of cerebellar granule neurons transiently transfected with designated filamin A (F1) or scr siRNA oligonucleotide was quantified and normalized to control levels (means ± s.d.; n=4; $^{***}P$<0.001). (J) Viability of neurons expressing designated filamin A or scr siRNA (means ± s.d.; n=4). Scale bars: 20 μm.

Journal of Cell Science

even have a dominant inhibitory effect in neuronal migration. We currently do not have a good mechanistical explanation for this. In theory, it could be, for example, due to FD-IKAP titrating out components needed for migration, especially in cells with low levels of wild-type IKAP. Based on these observations, it is evident that the expression and stability of FD-IKAP, especially in the sensory and autonomous nervous systems, should be thoroughly investigated in order to understand the aetiology of FD as well as for planning for efficient treatment strategies. This would require development of new anti-N-terminal-IKAP antibodies that are efficient in western blot analysis.

In a recent publication (Close et al., 2006), IKAP depletion using a single RNAi sequence against *IKBKAP* was shown to result in downregulation of the expression of a specific set of genes leading to a migration defect. This is consistent with the previous publications of the role of IKAP/Elp1 in transcriptional elongation (Otero et al., 1999; Hawkes et al., 2002). Surprisingly, by using both siRNA and shRNA technology, and several different RNAi sequences against *IKBKAP*, we did not observe downregulation of paxillin and beclin 1, two main transcriptional elongation targets of IKAP, described in the earlier study (Close et al., 2006). Expression array analysis of genes involved in cellular adhesion and migration did not show any clear transcriptional differences either. This major discrepancy between these two studies could simply just be due to functional differences between the RNAi sequences used in this study and the single RNAi sequence (5′-TCCTCAGTGCTTCTCTCTC-3′; published here with a kind permission from A. Chariot, Laboratory of Medical Chemistry/CTCM/CBIG Tour de Pathologie, Liege, Beglium) used in the previous study. It is very likely also that cells are able to compensate at the protein level for the possible transcriptional defects of paxillin and beclin 1 that are mediated by IKAP depletion, especially if the transcriptional changes are not very prominent. The previous study reported lower paxillin and beclin 1 levels in an FD-patient fibroblast cell line compared with a control-individual cell line (Close et al., 2006). Again, we could not find any differences in the protein levels of paxillin and beclin 1 using a patient-fibroblast cell line and a healthy-individual sample available in our laboratory, suggesting that the lower paxillin and beclin 1 mRNA expression levels in the patient fibroblasts could be compensated for at the protein level. Interestingly, an expression array analysis of cerebrum of two FD patients did not reveal differences in paxillin or beclin 1 expression in comparison to healthy individuals. Instead, at least twofold downregulation were observed in the expression of several genes involved in oligodendrocyte differentiation and myelination (Cheishvili et al., 2007).

How could the interaction of IKAP and filamin A regulate cytoskeleton organization? The data obtained thus far suggest a model in which the association of IKAP and filamin A is mediated via a third unknown association partner. Via its association partner, IKAP assists the localization of filamin A in the membrane ruffles upon cell migration. This function of IKAP is mediated via the C-terminal part of IKAP, because ectopic expression of N-terminal FD-IKAP could not assist filamin A localization to membrane ruffles. Furthermore, introduction of human cIKAP into IKAP-downregulated MEFs partially rescued the migration defect (data not shown), supporting this notion. Two of the most obvious candidates for an IKAP association partner are ELP2 and ELP3, which both reside in the cytosol. Interestingly, depletion of IKAP has been shown to destabilize ELP3, supporting the idea of their functional connection (Close et al., 2006). Despite various efforts, we did not, however, manage to deplete ELP3. It would be of interest to stain migrating cells with antibodies against ELP2 and ELP3 to find out if they can also localize to membrane ruffles. However, for this, the development of new efficient antibodies against human ELP2 and ELP3 would be needed.

In this work, we provide evidence for the central role of the cytosolic pool of IKAP in cell adhesion, migration and actin cytoskeleton organization. The results support a model in which IKAP-assisted sub-cellular localization of filamin A regulates cell migration. Here, we show that the N-terminal fragment of *IKBKAP*, FD-*IKBKAP*, can be translated into a stable protein that is, however, missing the migration-supporting function of IKAP. We also demonstrate for the first time a defect in the migration of primary neurons upon IKAP depletion as well as following expression of FD-IKAP. Together, the data presented suggest a novel model that illustrates how loss-of-function of IKAP could lead to neuronal-migration defects, which in turn could contribute to FD. The novel data presented here can be highly relevant for understanding the disease mechanism behind FD as well as for planning the treatment strategies.

Materials and Methods

Antibodies

The following antibodies were used: anti-IKAP (clone 33, Transduction Laboratories); polyclonal anti-IKAP (071-FB) against the C-terminus of IKAP, provided by S. Slaugenhaupt (Center for Human Genetic Research, Boston, MA); polyclonal anti-IKAP (422) against the N-terminus (152-167) of IKAP; monoclonal anti-vinculin, anti-tubulin and anti-β-actin (Sigma); anti-filamin-A (MAB1678, Chemicon); anti-beclin-1 (BD Transduction Laboratories); monoclonal anti-GAPDH (Biogenesis); HRP-conjugated rabbit anti-mouse and swine anti-rabbit antibody (DakoCytomation); and Alexa-Fluor-488-conjugated goat anti-mouse, Alexa-Fluor-488- and -546-conjugated goat anti-rabbit, Alexa-Fluor-488-conjugated donkey anti-mouse and Alexa-Fluor-546-conjugated donkey anti-rabbit (Invitrogen). Anti-paxillin was used for immunostaining (Transduction Laboratories) and western blotting (clone 5H11, Upstate Biotechnology).

Cell culture

MEFs, Phoenix Eco and Ampho packaging cell lines (http://www.stanford.edu/group/nolan/retroviral_systems/phx.html), and HEK293 cells were cultured as in Fehrenbacher et al. (Fehrenbacher et al., 2004). Human 3652 fibroblasts were cultured in DMEM (Sigma) and FD-patient and control-individual fibroblasts in RPMI (Sigma) supplemented with 20% FCS, 8 μg/ml non-essential amino acids (NEA), and 100 U/ml penicillin and streptomycin. HeLa cells were grown in RPMI supplemented with 6% FCS, and 100 U/ml penicillin and streptomycin. Cerebellar granule neurons were prepared from postnatal day 7 Sprague Dawley rats and cultured as in Coffey et al. (Coffey et al., 2000).

Constructs and siRNA oligonucleotides

shRNAs against murine and human *IKBKAP*, and a scrambled control, were cloned into the retroviral vector pSUPER.retro (Oligoengine). siRNA oligonucleotides against human and rat *IKBKAP* and rat filamin A (5′-CTACCTACTTTGAGATCTT-3′) and a scrambled control were purchased from Dharmacon. *IKBKAP* RNAi sequences are presented in supplementary material Fig. S1. Human *IKBKAP* (Holmberg et al., 2002) and FD-*IKBKAP* (bp 1-2142) were cloned into the pBabe retroviral vector. 102-*IKBKAP*-His, GFP-*IKBKAP* and His-*IKBKAP* were as described in Holmberg et al. (Holmberg et al., 2002). For cIKAP-strep, cIKAP (bp 2143-3996) was amplified by PCR (oligonucleotide sequences are available upon request) and cloned into *Bsa*I sites in the pEXPR-IBA105-vector. For FD-*IKBKAP*-GFP, the corresponding cDNA was amplified and cloned into eGFP-N1 vector (Invitrogen). Filamin A construct was provided by Thomas Stossel (Leonardi et al., 2000).

Retroviral expression of shRNAs and western blotting analysis

The retroviral infections and western blotting analysis were performed as in Dietrich et al. (Dietrich et al., 2004).

Transient transfection

HeLa cells were transfected with 1.5 μg/ml of GFP-constructs or 50 nM of designated siRNAs using FuGeneHD (Roche) or Oligofectamine (Invitrogen), respectively.

Real-time and reverse-transcriptase PCR

RNA was isolated with RNeasy RNA isolation kit (Qiagen) and cDNA was synthesized with Taqman RT kit (Roche). Rat SCG neurons were cultured for 24

Journal of Cell Science

hours in the presence of 100 ng/ml CNTF and cDNA was prepared as described previously (Wyttenbach and Tolkovsky, 2006). *VIP* primers are described elsewhere (Fann and Patterson, 1993). Mouse-brain cDNA was from Clontech. RT-PCR analysis was performed with FastStart+ SyBR Green I Mastermix (Roche) in a Light Cycler 2.0 (Roche). The expression level of *IKBKAP* was normalized to the expression level of the housekeeping gene PBGD. Oligonucleotide sequences and PCR conditions are available upon request.

Cytotoxicity assay

Cytotoxicity was analyzed with an LDH cytotoxicity kit (Roche).

Immunofluorescence microscopy

Cells were fixed 10 minutes in methanol or 30 minutes in 3.7% paraformaldehyde followed by permeabilization in 0.1% Triton-X-100 for 3 minutes. Blocking was performed in 5% serum. Alexa-Flour-488 or -546-conjugated phalloidin (Molecular Probes) was included in the last wash for 20 minutes at 20°C to stain the actin cytoskeleton. Visualization was performed on a Zeiss Axiovert 100M confocal microscope. Quantification of the cells with organized paxillin and actin or filamin A localization to membrane ruffles was calculated by counting at least 50 cells in each sample.

Preparation of cytosolic and nuclear extracts, One-STrEP-tag purification and co-immunoprecipitation

HEK293 cells were transiently transfected as indicated and harvested 2 days after. Cytosolic extracts were prepared by re-suspending the cells in hypotonic buffer A for 20 minutes on ice (10 mM HEPES, pH 7, 10 mM KCl, 0.1 mM EDTA, 0.1 mM EGTA, 0.1% NP-40, 1.5 mM $MgCl_2$) and collecting the supernatant after centrifuging 3 minutes at 3900 ***g***. The pellet was washed once and resuspended in Solution 2 (20 mM HEPES, pH 7.9, 400 mM NaCl, 0.25 mM EGTA, 1.5 mM $MgCl_2$, 10% glycerol) for 20 minutes on ice and centrifuged for 3 minutes at 3900 ***g*** to prepare nuclear extract. One-STrEP-tag purification was performed according to the manufacturer's instructions (IBA, Germany). For co-immunoprecipitation, Tris-HCl, NaCl and NP-40 were added to the lysates to achieve the following conditions: 10 mM Tris-HCl, pH 7.4, 150 mM NaCl, 0.2% NP-40.

Soluble and insoluble actin measurement

Cells were washed with PBS and extracted for 3 minutes with pre-warmed (37°C) PEM buffer (100 mM Pipes, pH 6.9, 1 mM $MgCl_2$, 1 mM EGTA) containing 0.75% TX100. Supernatant (soluble actin) was collected and the remaining cells were washed with pre-warmed PEM and lysed directly into an equal amount of loading buffer to give the insoluble actin. Equal volumes of each fraction were loaded on SDS-PAGE and blotted for β-actin.

Protein identification by mass spectrometry

Protein spots of interest were excised from the dry silver-stained gels and prepared as described previously (Shevchenko et al., 1996). Mass spectrometry was performed using a Reflex IV MALDI-TOF mass spectrometer equipped with a Scout 384 ion source as described previously (Celis et al., 2004).

Neuronal migration analysis

Cerebellar granule neurons were plated on 0.33 cm^2 Transwells (Corning) coated with laminin (10 μg/ml). Cells were transfected as previously described (Coffey et al., 2000) with 100 nM of the indicated siRNA together with 1 μg of pEGFP. After 48 hours, cells were fixed and EFGP-expressing cells that had migrated through the membrane were counted. Neuronal viability was determined from Hoechst-33342-stained nuclei. Cells with pyknotic nuclei were scored dead.

Supplemental material

As shown in the supplementary material, the human extracellular matrix and adhesion molecules RT^2 profiler PCR array (SuperArray) was used to investigate differences in expression of 84 genes important for cell-cell and cell-matrix interactions. Total RNA was isolated from cells with RNeasy RNA isolation kit (Qiagen) and used for single-stranded cDNA synthesis with Taqman RT kit (Roche). Analysis of two sets of vector-control and h1 shRNA cells was performed according to the manufacturer's instructions. PI staining of cells for flow cytometry was performed on adhered (2-3 days after plating), 50% confluent cells. Cells were fixed with 70% ice-cold methanol and suspended into PI-buffer (10 mM Tris-HCl, pH 7.5, 5 mM $MgCl_2$, 50 μg PI/ml and 10 μg of DNase-free RNase/ml) and subjected to flow cytometry (FACScalibur, Becton Dickinson).

This work was supported by the Dysautonomia Foundation Inc. (T.K.), Bøje Benzon stipend of Alfred Benzon Foundation (T.K.), the Danish Cancer Society (T.K., M.J.), the Danish Medical Research Council (T.K.), the Danish National Research Foundation (M.J.), the Meyer Foundation (M.J.), the Novo Foundation (T.K.), the Academy of Finland (E.T.C.), Turku University Biomedical Sciences Graduate School (N.W.) and the Wellcome Trust (A.T). We thank Susan Slaugenhaupt, Kristian Helin, Adrian Bracken, Mette Hartvig Jensen and Timo Pikkarainen for valuable tools and advice.

References

Abassi, Y. A., Rehn, M., Ekman, N., Alitalo, K. and Vuori, K. (2003). p130Cas Couples the tyrosine kinase Bmx/Etk with regulation of the actin cytoskeleton and cell migration. *J. Biol. Chem.* **278**, 35636-35643.

Anderson, S. L., Coli, R., Daly, I. W., Kichula, E. A., Rork, M. J., Volpi, S. A., Ekstein, J. and Rubin, B. Y. (2001). Familial dysautonomia is caused by mutations of the IKAP gene. *Am. J. Hum. Genet.* **68**, 753-758.

Axelrod, F. B. (2004). Familial dysautonomia. *Muscle Nerve* **29**, 352-363.

Celis, J. E., Gromov, P., Cabezon, T., Moreira, J. M., Ambartsumian, N., Sandelin, K., Rank, F. and Gromova, I. (2004). Proteomic characterization of the interstitial fluid perfusing the breast tumor microenvironment: a novel resource for biomarker and therapeutic target discovery. *Mol. Cell. Proteomics* **3**, 327-344.

Cheishvili, D., Maayan, C., Smith, Y., Ast, G. and Razin, A. (2007). IKAP/hELP1 deficiency in the cerebrum of familial dysautonomia patients results in down regulation of genes involved in oligodendrocyte differentiation and in myelination. *Hum. Mol. Genet.* **16**, 2097-2104.

Close, P., Hawkes, N., Cornez, I., Creppe, C., Lambert, C. A., Rogister, B., Siebenlist, U., Merville, M. P., Slaugenhaupt, S. A., Bours, V. et al. (2006). Transcription impairment and cell migration defects in elongator-depleted cells: implication for familial dysautonomia. *Mol. Cell* **22**, 521-531.

Coffey, E. T., Hongisto, V., Dickens, M., Davis, R. J. and Courtney, M. J. (2000). Dual roles for c-Jun N-terminal kinase in developmental and stress responses in cerebellar granule neurons. *J. Neurosci.* **20**, 7602-7613.

Cohen, L., Henzel, W. J. and Baeuerle, P. A. (1998). IKAP is a scaffold protein of the IkappaB kinase complex. *Nature* **395**, 292-296.

Collum, R. G., Brutsaert, S., Lee, G. and Schindler, C. (2000). A Stat3-interacting protein (StIP1) regulates cytokine signal transduction. *Proc. Natl. Acad. Sci. USA* **97**, 10120-10125.

Cuajungco, M. P., Leyne, M., Mull, J., Gill, S. P., Lu, W., Zagzag, D., Axelrod, F. B., Maayan, C., Gusella, J. F. and Slaugenhaupt, S. A. (2003). Tissue-specific reduction in splicing efficiency of IKBKAP due to the major mutation associated with familial dysautonomia. *Am. J. Hum. Genet.* **72**, 749-758.

Cunningham, C. C., Gorlin, J. B., Kwiatkowski, D. J., Hartwig, J. H., Janmey, P. A., Byers, H. R. and Stossel, T. P. (1992). Actin-binding protein requirement for cortical stability and efficient locomotion. *Science* **255**, 325-327.

Dietrich, N., Thastrup, J., Holmberg, C., Gyrd-Hansen, M., Fehrenbacher, N., Lademann, U., Lerdrup, M., Herdegen, T., Jaattela, M. and Kallunki, T. (2004). JNK2 mediates TNF-induced cell death in mouse embryonic fibroblasts via regulation of both caspase and cathepsin protease pathways. *Cell Death Differ.* **11**, 301-313.

Dujardin, D. L., Barnhart, L. E., Stehman, S. A., Gomes, E. R., Gundersen, G. G. and Vallee, R. B. (2003). A role for cytoplasmic dynein and LIS1 in directed cell movement. *J. Cell Biol.* **163**, 1205-1211.

Esberg, A., Huang, B., Johansson, M. J. and Bystrom, A. S. (2006). Elevated levels of two tRNA species bypass the requirement for elongator complex in transcription and exocytosis. *Mol. Cell* **24**, 139-148.

Fann, M. J. and Patterson, P. H. (1993). A novel approach to screen for cytokine effects on neuronal gene expression. *J. Neurochem.* **61**, 1349-1355.

Fehrenbacher, N., Gyrd-Hansen, M., Poulsen, B., Felbor, U., Kallunki, T., Boes, M., Weber, E., Leist, M. and Jaattela, M. (2004). Sensitization to the lysosomal cell death pathway upon immortalization and transformation. *Cancer Res.* **64**, 5301-5310.

Feng, Y. and Walsh, C. A. (2004). The many faces of filamin: a versatile molecular scaffold for cell motility and signalling. *Nat. Cell Biol.* **6**, 1034-1038.

Fox, J. W., Lamperti, E. D., Eksioglu, Y. Z., Hong, S. E., Feng, Y., Graham, D. A., Scheffer, I. E., Dobyns, W. B., Hirsch, B. A., Radtke, R. A. et al. (1998). Mutations in filamin 1 prevent migration of cerebral cortical neurons in human periventricular heterotopia. *Neuron* **21**, 1315-1325.

Friocourt, G., Kappeler, C., Saillour, Y., Fauchereau, F., Rodriguez, M. S., Bahi, N., Vinet, M. C., Chafey, P., Poirier, K., Taya, S. et al. (2005). Doublecortin interacts with the ubiquitin protease DFFRX, which associates with microtubules in neuronal processes. *Mol. Cell. Neurosci.* **28**, 153-164.

Habecker, B. A., Asmus, S. A., Francis, N. and Landis, S. C. (1997). Target regulation of VIP expression in sympathetic neurons. *Ann. N. Y. Acad. Sci.* **814**, 198-208.

Hatten, M. E. (1990). Riding the glial monorail: a common mechanism for glial-guided neuronal migration in different regions of the developing mammalian brain. *Trends Neurosci.* **13**, 179-184.

Hawkes, N. A., Otero, G., Winkler, G. S., Marshall, N., Dahmus, M. E., Krappmann, D., Scheidereit, C., Thomas, C. L., Schiavo, G., Erdjument-Bromage, H. et al. (2002). Purification and characterization of the human elongator complex. *J. Biol. Chem.* **277**, 3047-3052.

Hims, M. M., Shetty, R. J., Pickel, J., Mull, J., Leyne, M., Liu, L., Gusella, J. F. and Slaugenhaupt, S. A. (2007). A humanized IKBKAP transgenic mouse models a tissue-specific human splicing defect. *Genomics* **90**, 389-396.

Holmberg, C., Katz, S., Lerdrup, M., Herdegen, T., Jaattela, M., Aronheim, A. and Kallunki, T. (2002). A novel specific role for I kappa B kinase complex-associated protein in cytosolic stress signaling. *J. Biol. Chem.* **277**, 31918-31928.

Junttila, M. R., Saarinen, S., Schmidt, T., Kast, J. and Westermarck, J. (2005). Single-step Strep-tag purification for the isolation and identification of protein complexes from mammalian cells. *Proteomics* **5**, 1199-1203.

Kiema, T., Lad, Y., Jiang, P., Oxley, C. L., Baldassarre, M., Wegener, K. L., Campbell, I. D., Ylänne, J. and Calderwood, D. A. (2006). The molecular basis of filamin binding to integrins and competition with talin. *Mol. Cell* **21**, 337-347.

Krogan, J. N., Kim, M., Ahn, S. H., Zhong, G., Kobor, M. S., Cagney, G., Emili, A., Shilatifard, A., Buratowski, S. and Greenblatt, J. F. (2002). RNA polymerase II elongation factors of Saccharomyces cerevisiae: a targeted proteomics approach. *Mol. Cell. Biol.* **22**, 6979-6992.

Leonardi, A., Ellinger-Ziegelbauer, H., Franzoso, G., Brown, K. and Siebenlist, U. (2000). Physical and functional interaction of filamin (actin-binding protein-280) and tumor necrosis factor receptor-associated factor 2. *J. Biol. Chem.* **275**, 271-278.

Otero, G., Fellows, J., Li, Y., de Bizemont, T., Dirac, A. M., Gustafsson, C. M., Erdjument-Bromage, H., Tempst, P. and Svejstrup, J. Q. (1999). Elongator, a multisubunit component of a novel RNA polymerase II holoenzyme for transcriptional elongation. *Mol. Cell* **3**, 109-118.

Pokholok, D. K., Hannett, N. M. and Young, R. A. (2002). Exchange of RNA polymerase II initiation and elongation factors during gene expression in vivo. *Mol. Cell* **9**, 799-809.

Popowicz, G. M., Schleicher, M., Noegel, A. A. and Holak, T. A. (2006). Filamins: promiscuous organizers of the cytoskeleton. *Trends Biochem. Sci.* **31**, 411-419.

Rahl, P. B., Chen, C. Z. and Collins, R. N. (2005). Elp1p, the yeast homolog of the FD disease syndrome protein, negatively regulates exocytosis independently of transcriptional elongation. *Mol. Cell* **17**, 841-853.

Rakic, P., Stensas, L. J., Sayre, E. and Sidman, R. L. (1974). Computer-aided three-dimensional reconstruction and quantitative analysis of cells from serial electron microscopic montages of foetal monkey brain. *Nature* **250**, 31-34.

Sasaki, S., Shionoya, A., Ishida, M., Gambello, M. J., Yingling, J., Wynshaw-Boris, A. and Hirotsune, S. (2000). A LIS1/NUDEL/cytoplasmic dynein heavy chain complex in the developing and adult nervous system. *Neuron* **28**, 681-696.

Shevchenko, A., Wilm, M., Vorm, O. and Mann, M. (1996). Mass spectrometric sequencing of proteins silver-stained polyacrylamide gels. *Anal. Chem.* **68**, 850-858.

Slaugenhaupt, S. A., Blumenfeld, A., Gill, S. P., Leyne, M., Mull, J., Cuajungco, M. P., Liebert, C. B., Chadwick, B., Idelson, M., Reznik, L. et al. (2001). Tissue-specific expression of a splicing mutation in the IKBKAP gene causes familial dysautonomia. *Am. J. Hum. Genet.* **68**, 598-605.

Slaugenhaupt, S. A., Mull, J., Leyne, M., Cuajungco, M. P., Gill, S. P., Hims, M. M., Quintero, F., Axelrod, F. B. and Gusella, J. F. (2004). Rescue of a human mRNA splicing defect by the plant cytokinin kinetin. *Hum. Mol. Genet.* **13**, 429-436.

Vadlamudi, R. K., Li, F., Adam, L., Nguyen, D., Ohta, Y., Stossel, T. P. and Kumar, R. (2002). Filamin is essential in actin cytoskeletal assembly mediated by p21-activated kinase 1. *Nat. Cell Biol.* **4**, 681-690.

Wyttenbach, A. and Tolkovsky, A. M. (2006). The BH3-only protein Puma is both necessary and sufficient for neuronal apoptosis induced by DNA damage in sympathetic neurons. *J. Neurochem.* **96**, 1213-1226.

Journal of Cell Science